Trimethylaluminum: A Computer Study of the Condensed Phases and the Gas Dimer

Sundaram Balasubramanian,* Christopher J. Mundy, and Michael L. Klein

Center for Molecular Modeling and Department of Chemistry, University of Pennsylvania, Philadelphia, Pennsylvania 19104-6323

Received: May 19, 1998

Molecular dynamics simulations on trimethylaluminum, $Al(CH_3)_3$ (TMA), have been carried out to investigate the properties of the gas-phase dimer, the liquid, and the solid. An empirical potential model, suitable for classical simulations, has been developed. The empirical potential model captures the essential structural properties of TMA in the condensed phases and obtains fair agreement with experiments on the dimer vibrational properties. However, ab initio density functional theory based Car-Parrinello molecular dynamics simulations, performed on the TMA dimer, provide a much better representation of structural and vibrational features than the empirical model.

1. Introduction

Trimethylaluminum, $Al(CH_3)_3$ (TMA), is an exceptionally important organometallic compound to the chemical industry.[1] It is used as a cocatalyst for polymerization of alkenes in conjunction with homogeneous Ziegler−Natta catalysts such as halides of titanium or vanadium.[2] Further, research over the last two decades has shown that alkylaluminums are also active as cocatalysts along with aluminoxanes in polymerization reactions catalyzed by metallocenes.[3,4]

The monomeric TMA has only six electrons in its valence shell and is thus electron-deficient. This deficiency drives it to dimerize so that an eight electron configuration can be achieved.[5] It is known to be dimerized in the solid state,[6,7] in solution (with solvents such as benzene or cyclopentane),[8,9] and to a large extent in the gas phase.[10] The enthalpy of dimerization obtained from vapor pressure studies has been found to be 84.5 kJ/mol.[10] Pitzer and Gutowsky[9] have reported that while TMA is dimerized in solution, the ethyl and *n*-propyl analogues dissociate to some extent and triisopropylaluminum exists as monomers. TMA is thus a Lewis acid and is able to add to alkenes and alkynes in a process called "carbalumination".[11] Thus, as the organic ligand gets bulky, steric hindrance seems to play a large role in decreasing the stability of the dimer.

There are crucial differences between the structure of a TMA monomer as opposed to that of the dimer[12] (see Figure 1). For the purposes of this article, we denote the methyl groups bridging two aluminum atoms in a dimer as C_b, while the terminal methyl groups are denoted by C_t. The monomer has D_{3h} symmetry with the angle C−Al−C being 120°. In the dimer, the angle C_t-Al-C_t is ca. 117°, close to the angle in the monomer, and representative of sp^2 hybridization. But the angle formed by the bridging carbons, C_b-Al-C_b, is ca. 105°, closer to sp^3 hybridization. Thus, the nature of bonding in TMA dimer is likely to have characteristics of both types of hybridization.[1] Another feature to note in the dimer is that the central $Al-C_b-Al-C_b$ bridge is nearly planar and is perpendicular to the two C_t-Al-C_t planes.

Proton and ^{13}C nuclear magnetic resonance (NMR) experiments performed on TMA in solution, at temperatures below ambient conditions, exhibit one peak only.[13,14] This is interpreted as being due to the rapid (faster than NMR time scales) exchange of terminal and bridging methyl groups. From the temperature dependence of the line width of this resonance, Ramey et al.[14] calculated an activation enthalpy for this exchange process to be 65 kJ/mol. The vibrational properties have also been studied by infrared (IR) and Raman spectroscopic measurements.[15] Onishi and Shimanouchi[16] performed a normal-mode analysis of the TMA dimer based on a Urey−Bradley force field to assign the spectra.

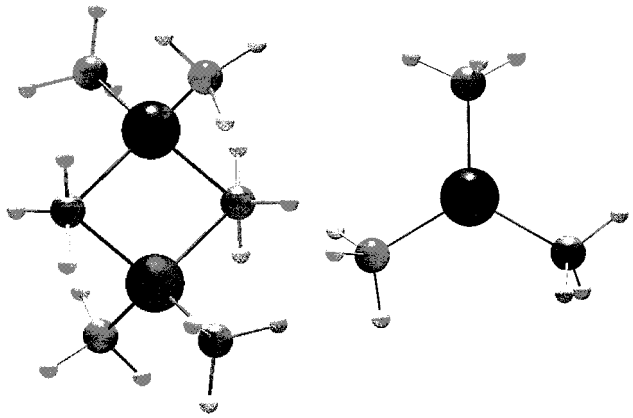

Figure 1. Structure of TMA dimer and monomer determined by electron diffraction.[12]

Despite having an important role in polymerization reactions, very few modeling studies have been reported on TMA. Previous work has included Hartree−Fock calculations on TMA and its complexes with alkenes.[17] More recently, Tarazona et al.[18] employed Hartree−Fock calculations to obtain the structural and far-infrared features of dimers of TMA, $AlCl_3$, and various mixed systems. They also reported some density functional theory based Car-Parrinello ab initio molecular dynamics simulations, which suggested that the TMA dimer was unstable to thermal motion.

The present article details an attempt to derive an empirical model for TMA using a classical force field. Empirically derived classical potentials are quite useful in understanding the gross structural and dynamical features of complex systems, particularly in condensed phases. But the fine details of the structure in a system such as TMA are likely to be borne out only in ab

10.1021/jp982291s CCC: $15.00
Published on Web 11/19/1998

initio simulations, which being expensive have limitations on the sizes of systems that can be studied. It is thus important that suitable empirical potential models are obtained for these organometallics so that representative atomic configurations from a classical trajectory can also serve as starting points for refined studies where the potentials are less empirically derived.

The present work is intended to complement experimental data and spur further interest in studying the condensed phases of these strongly bonded materials. Anticipating our results, we find that our classical model fares reasonably well in reproducing structural data on TMA in its condensed phases. However for the vibrational properties of the dimer, the model needs further improvement. We have also employed the Car-Parrinello molecular dynamics (CPMD) method on the gas-phase dimer of TMA and find, in contrast to earlier work,[18] that the results agree rather well with experimental data.

This article is divided into the following sections. In the next section, the development of the classical empirical potential model for TMA is presented. In section 3 the details of the simulation methods used are discussed. Section 4 contains the results from both the classical MD simulations and ab initio CPMD on the dimer. Conclusions derived from this work are presented in section 5.

2. Potential Model

Our goal is to develop a simple empirical potential model for TMA that can be used to study bond formation and breaking and, thus, to allow for the monomer−dimer equilibrium, which is observed experimentally in the gas phase. Ideally, the potential model should also be transferable to condensed phases.

The model we chose assumes TMA to be composed of aluminum atoms and rigid methyl groups, whose interaction potential is represented as

$$V(r_{ij}) = A_{ij}\exp(-B_{ij}r_{ij}) + \frac{1}{4\pi\epsilon_0}q_iq_je^2/r_{ij} - C_{ij}/r_{ij}^{\,6} \quad (1)$$

The methyl groups contain hydrogen atoms. In eq 1, i and j denote interaction sites, A_{ij} and B_{ij} characterize the repulsive interactions, while C_{ij} is the dispersion constant. Apart from these interactions, the atoms carry a charge denoted by q_i. In assuming a potential of this form, we have explicitly neglected the effects of polarizability on the Al−C bond. The limitations of this simplifying assumption can be seen from the structure of the TMA dimer shown in Figure 1. There are actually two distinct Al−C distances in TMA, Al−C_b and Al−C_t. This distinction is not reflected in the primitive nonpolarizable interaction model. Our aim in this article is thus confined to exploring the capacity of this model to represent the gross properties of TMA. Several possible methods for systematically improving upon this scheme have been outlined in the literature[19,20] and will form the basis for future studies. In arriving at values for the potential parameters, we used the following relation to obtain their initial estimates.[21]

$$A_{ij} = f_0(b_i + b_j)\exp[(a_i + a_j)/(b_i + b_j)]$$
$$B_{ij} = 1/(b_i + b_j)$$
$$C_{ij} = c_ic_j \quad (2)$$

Here, a_i denotes the effective radius of atom i and b_i is the hardness parameter. The parameters for aluminum were obtained from an earlier work on aluminophosphates,[22] and those for carbon and hydrogen were adopted from the work of Williams.[23]

TABLE 1: Atomic Parameters for Eq 2 Used To Obtain Initial Estimates of the Potential Parameters Found in Table 2

atom	a [Å]	b [Å]	c [K$^{1/2}$ Å^3]
Al	0.95	0.032	955.5
C	1.75	0.139	534.5
H	1.23	0.135	116.6

TABLE 2: Parameters for the Potential Described in Eq 1 for TMA[a]

pair	A_{ij} [K]	B_{ij} [Å^{-1}]	C_{ij} [KÅ^6]
Al−Al	2.518e+14	10.925	20.13e+05
Al−C	6.195e+08	5.948	5.108e+05
Al−H	3.923e+07	5.988	1.115e+04
C−C	4.207e+07	3.597	2.860e+05
C−H	7.276e+06	3.649	6.236e+04
H−H	1.231e+06	3.704	1.361e+04

[a] The charges (q) on aluminum and carbon atoms were 1.2e and −0.4e, respectively, where e is the electronic charge. The hydrogen atoms were neutral.

These initial estimates are tabulated in Table 1. f_0 was chosen to be 4.184 kJ/mol, following ref 21. As the charges employed in ref 22 do not provide neutrality for a system such as Al_2O_3, we had to come up with a set of charges specific to TMA. These charges were arrived at by trial and error by performing molecular dynamics runs for TMA in the gas and crystalline phases, until reasonable convergence with experimental data on the structure was obtained. The final interaction parameters are presented in Table 2. We point out that only three of these parameters (specifically, B_{Al-Al}, C_{Al-Al}, and B_{Al-C}) have changed from the estimated values obtained using eq 2 and atomic parameters tabulated in Table 1.

The minimum in the resulting Al−C potential is at 1.83 Å, with a bond energy of 381 kJ/mol. Although this is 35% larger than the mean bond enthalpy of 274 kJ/mol obtained from experiments,[11] results on physical properties obtained in the condensed state (see below) agree surprisingly well with experiments. We were unable to devise model potentials with Al−C bond energies comparable to experiment that were also able to reproduce the known density of the liquid. This limitation is the price to pay for a nonpolarizable model. As noted above, several possible schemes exist that might be utilized to systematically improve the present model.[19,20]

3. MD Calculations

Empirical Potential. For the classical MD simulations, the constraints on the geometry of the methyl groups were handled using the SHAKE/RATTLE/ROLL algorithm.[24] The C−H distances were constrained to 1.10 Å and the H−C−H angle to 109.47°. Details of the classical simulation methodology employed in this article can be found in ref 24. Periodic boundary conditions were applied in all three directions. The potential, eq 1 was cut off radially at 9.5 Å, but the ion−ion interactions were handled using the Ewald summation technique. Simulations of one TMA dimer were performed in a cubic box of linear dimension 25 Å under constant volume and temperature conditions. The simulations of liquid TMA were performed under isotropic constant pressure and constant temperature conditions at a pressure of 1 bar and at four different temperatures, from 298.2 to 398.2 K. The run at 298.2 K was started from an arbitrary configuration (the aluminum and methyl groups occupying simple cubic lattice positions) of 50 Al atoms and 150 methyl groups. Simulations at higher temperatures were initiated from the final configurations of runs of immediately lower temperature.

Constant pressure simulations in a MD cell where the cell angles and lengths can change independently (isothermal−isobaric ensemble) were performed to study the stability of the simulated TMA crystal at 223.2 K. The crystal structure of TMA was solved first by Lewis and Rundle[6] and was refined later by Vranka and Amma.[7] TMA crystals are monoclinic with eight monomers in a unit cell. The initial atomic coordinates and simulation box parameters for our simulation were chosen to match the crystallographic data of Vranka and Amma[7] obtained at 223.2 K. The smallest cell length is *b*, which is 6.96 Å. Our simulation box consisted of $2 \times 3 \times 2$ unit cells along the three axes, so that a spherical cutoff of 9.5 Å could be used. The simulated system contained 1248 atoms. As the hydrogen coordinates were not reported in ref 7, the hydrogen atoms were placed 1.10 Å away from the carbons, with a tetrahedral H−C−H angle. The initial orientation of all the methyl groups in the crystal were chosen to be the same. The crystal was first equilibrated under constant NVT conditions for 6 ps before starting the run under constant pressure. The equations of motion were integrated reversibly with a time step of 3 fs.[24] Simulations of the liquid were performed for over 300 ps after adequate equilibration times, and similar run lengths were used to study the crystal.

Ab Initio Dimer Studies. Ab initio CPMD[25−28] was employed to study the properties of the TMA dimer. Although other ab initio schemes exist and are useful, e.g. Hartree−Fock based methods,[17,18] we choose the CPMD method for its ability to generate a continuous dynamical trajectory at a given temperature. The dynamics, energetics, structure, and vibrational properties of the TMA dimer were then studied within the pseudopotential approximation of the Troullier−Martins type.[29] Spin-independent, gradient-corrected exchange and correlation functionals of the Becke−Lee−Yang−Parr variety[30,31] were used. An energy cutoff of 60 Ry was used to expand the orbitals in a plane wave basis set. The equations of motion were integrated with a time step of 0.1 fs. Three-dimensional periodic boundary conditions in a cubic box of linear dimension 14 Å were used. The energy-minimized structure of TMA dimer was annealed at 400 K prior to the CPMD run. During this procedure, each coefficient of the wave function was thermostated with a separate thermostat (the so-called "massive" thermostating scheme[32]) for 100 steps to ensure adequate equilibration. The temperature corresponding to the coefficients was set to 2×10^{-4} K. The ionic and the electronic degrees of freedom were coupled to Nosé−Hoover chain thermostats to control their temperature.[28] During the CPMD run, each state was thermostated independently while all the ionic degrees of freedom were coupled to one thermostat.

4. Results and Discussion

Classical MD Studies. The first exercise to test our potential was to find out if the TMA dimer geometry is produced via self-assembly from an arbitrary configuration of two Al atoms and six methyl groups. Indeed, we observed the spontaneous formation of the dimer within 50 ps. Figure 2 shows the final configuration of the dimer from such a MD run at 298.2 K. The structural data of the simulated TMA dimer is compared to electron diffraction results of TMA in the gas phase[12] and X-ray diffraction results obtained on the crystal[7] in Table 3. It is pertinent to note that the classical model fails to distinguish much between the Al−C_b and Al−C_t distances, although the connectivity of the TMA dimer is reproduced well.

Another crucial feature in the simulated dimer is that the Al−C_b−Al and C_b−Al−C_b angles are close to 90° instead of 76° and 104° observed experimentally. A better model than the one presently developed which incorporates polarizability effects will likely be able to address these concerns.[19] Despite these shortcomings, we have persevered with this model to perform simulations of TMA in its condensed states.

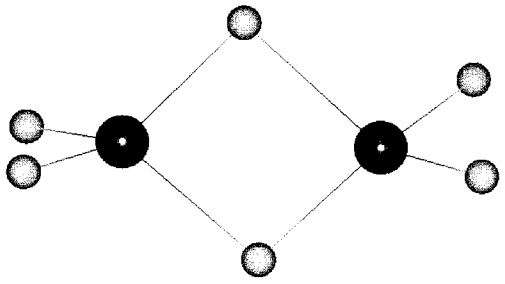

Figure 2. Final configuration of a TMA dimer, $(Al(CH_3)_3)_2$, formed out of a classical MD run with an arbitrary initial configuration of aluminum atoms and methyl groups. Hydrogen atoms are masked for clarity in this and the subsequent figures.

TABLE 3: Comparison of TMA Dimer Geometry Obtained from Simulations with Experiment[a]

	classical MD	CPMD	X-ray[7]	electron diffraction[12]
		Distance [Å]		
Al−Al	2.82	2.55	2.6	2.62
Al−C_b	1.99	2.09	2.14	2.14
Al−C_t	1.90	1.92	1.97	1.96
		Angle (deg)		
Al−C_b−Al	90.2	75.1	74.7	75.5
C_b−Al−C_b	88.1	104.9	105.3	104.5
C_t−Al−C_t	115.5	120.9	123.1	117.3
C_t−Al−C_b	112.2	107.5	106.8	

[a] Classical MD: MD performed at 298.2 K on one TMA dimer using the empirical potential, eq 1. CPMD: Energy-minimized structure of the TMA dimer using the Car-Parrinello method. X-ray: Diffraction data on TMA crystal at 223.2 K.[7] Electron diffraction: Data on gas-phase TMA dimer at 333.2 K.[12]

TABLE 4: Density of Liquid TMA at Different Temperatures

temp [K]	simulation [g/cm^3]	experiment[33] [g/cm^3]
298.2	0.74 ± 0.2	0.76
323.2	0.74 ± 0.2	0.73
348.2	0.71 ± 0.2	0.71
373.2	0.68 ± 0.2	0.70

Another important indicator of the efficacy of the potential is the energy of dimerization of TMA. As discussed earlier, TMA is found to be mostly dimeric in all phases and the enthalpy of dimerization from vapor pressure measurements was found to be 84.5 kJ/mol.[10] The classical model predicts a dimerization energy of 125 kJ/mol in favor of the dimer over the monomer in the gas phase. This is consistent with the higher Al−C bond energy of the model noted in section 2. The enthalpy of the dimer (or monomer) at 298.2 K has contributions other than the internal energy at the potential minimum. These include translational, rotational, vibrational and zero-point energy contributions. We estimate these to contribute around 10 kJ/mol to the dimerization energy in favor of the monomer.[17] Thus, we estimate the experimental dimerization energy to be around 95 kJ/mol, which is about 25% less than the value of the empirical potential.

Simulation results on the liquid-phase densities of TMA at four temperatures, averaged over 100 ps are presented in Table 4. Our average computed densities compare well with experiment at all temperatures,[33] suggesting that the thermal expansion coefficient of the liquid is reasonable.

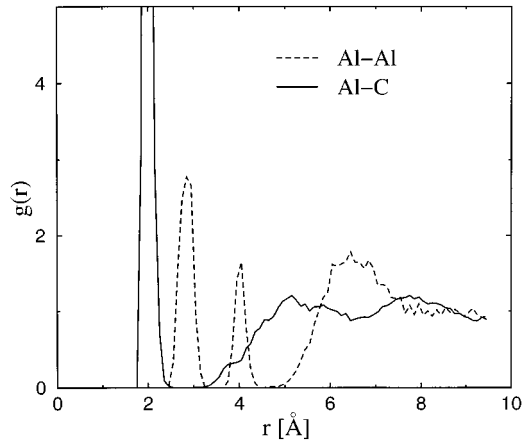

Figure 3. Pair correlation functions of Al−Al and Al−C in liquid TMA at 298.2 K.

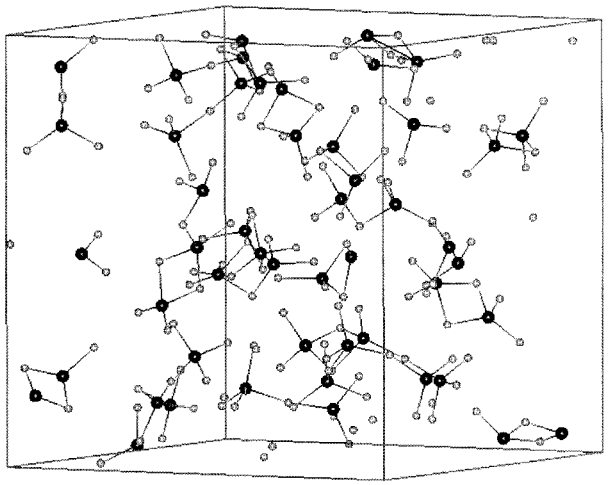

Figure 4. Snapshot of a configuration of TMA in the liquid phase at 298.2 K modeled using the classical potential (eq 1). The large and small spheres are aluminum and carbon atoms, respectively.

The liquid pair correlation function, $g(r)$ for Al−Al is shown in Figure 3 along with the corresponding $g(r)$ for Al−C. At 298.2 K, the latter exhibits a sharp peak around 2.0 Å. From this first coordination shell of carbon around aluminum, the number of closest carbons is found to be four. A measure of dimerization in liquid TMA can be obtained from the Al−Al coordination number, which shows that the present model is able to assemble TMA dimers out of aluminum atoms and methyl groups. The first coordination shell of Al−Al is 2.9 Å, and the coordination number is 0.70. This indicates that 70% of the aluminum atoms exist as dimers in the simulated liquid sample at 298.2 K. The ratio of dimers to monomers is only marginally affected by temperature. At 398.2 K, we find 64% of aluminum atoms as dimers. Interparticle distances are much less affected by temperature, in agreement with the notion that the TMA dimer is a relatively stable entity even in the gas phase. Using the distance criterion of 2.4 Å for the Al−C bond at 298.2 K, we find that 101 carbons are singly coordinated to Al and the rest are coordinated to two Al atoms, consistent with the geometry of TMA dimers. Integrating the C−C g(r) (not shown) until its first minimum, we find that four carbons surround a central carbon, again in agreement with the structure of the TMA dimer. The dimers can also be seen in a snapshot of the atomic configuration at 298.2 K shown in Figure 4.

A further test of the potential model comes from simulations on the TMA crystal. The cell parameters over the period of simulation are stable and are in reasonable agreement with

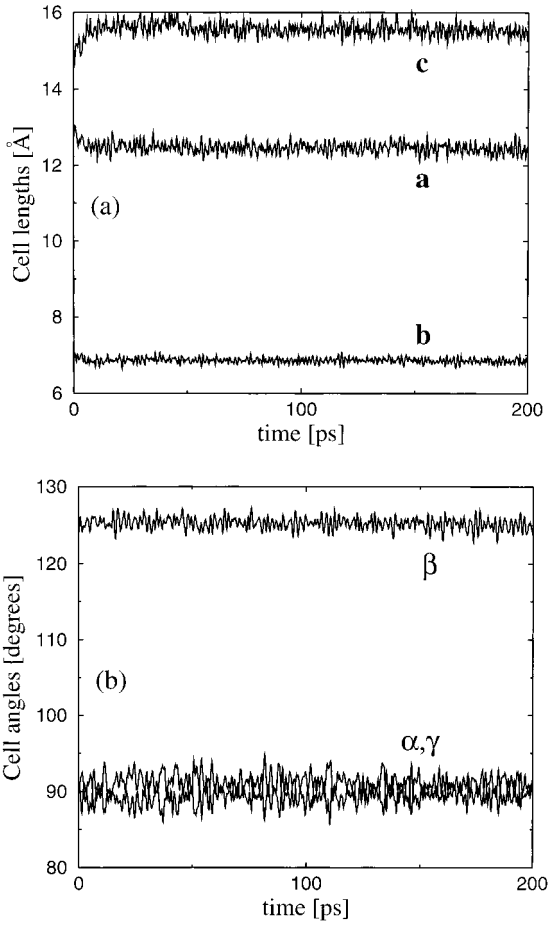

Figure 5. Plot of instantaneous cell parameters of the classically simulated TMA crystal at 223.2 K: (a) cell lengths; (b) cell angles.

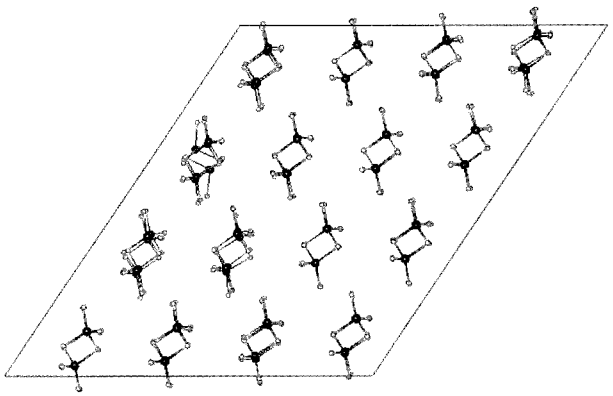

Figure 6. Averaged configuration of the classically simulated TMA crystal viewed along the *b* axis of the monoclinic unit cell.

experiment. These are shown in Figure 5. A configuration of the simulated crystal averaged over 100 ps is shown in Figure 6. Intermolecular order is well preserved, thus demonstrating that the potential reproduces a stable crystalline phase. Although one of the cell lengths (*c*) is different from experiment by about 6%, the density of the simulated crystal differs from the experimental value of 0.887 g/cm[37] by only 0.4%. The central bridge in the TMA dimer comprising $Al-C_b-Al-C_b$ atoms is found to largely planar, with the distribution of the torsional angle exhibiting a Gaussian form with the mean at 0° and a half-width at half-maximum of around 16°.

The IR and Raman spectra of TMA in solution have been studied extensively.[15,16] It is thus important to find out how well our model agrees with experiments on the vibrational properties.

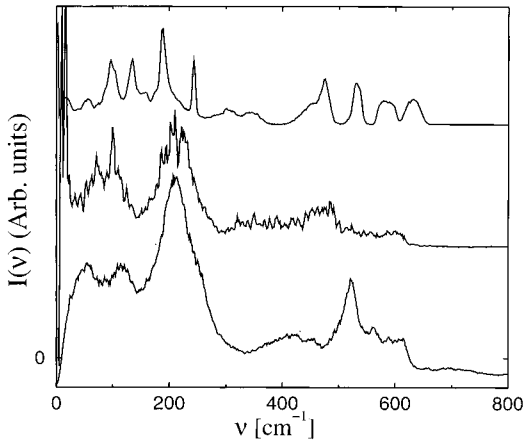

Figure 7. Power spectra of all the atoms in the classically modeled TMA crystal (bottom) and of the TMA dimer in the gas phase with flexible methyl groups (middle). The top graph is the frequency spectrum of the latter obtained at 5 K through a normal-mode analysis. The spectra were smoothed by a three-point sampling method.

The power spectrum of the velocity autocorrelation function of the atoms in the TMA crystal is shown in Figure 7. The spectrum exhibits features at frequencies that are comparable with those found in experiments, although some of the modes are shifted considerably in frequency.

To investigate the nature of atomic motions underlying the features in the power spectrum, we carried out a normal-mode analysis of the dynamics of the TMA dimer. To do so, we first obtain the force constant matrix[34]

$$F_{i\alpha j\beta} = \frac{\partial^2 V}{\partial q_{i\alpha} \partial q_{j\beta}} \tag{3}$$

where α and β refer to Cartesian coordinates, *x, y, z*. q_i denotes the mass-weighted coordinate of atom i, $q_i = m_i 1/2 r_i$. The frequencies of the normal modes are obtained from the eigenvalues, Λ_k of $\vec{\mathbf{F}}$ as $\omega_k{}^2 = \Lambda_k$. The eigenvectors represent atomic displacements in Cartesian coordinates.

As discussed in section 3A, our model involves rigid methyl groups that are handled by constraints. Thus, the values of those elements (degrees of freedom) of $\vec{\mathbf{F}}$ that are involved in the constraint will equal the Lagrange multiplier, λ, for the corresponding constraint. Since storing and analyzing these data is rather tedious, we have employed flexible methyl groups for purposes of this analysis alone. The flexible methyl groups had harmonic C−H stretch and H−C−H bending potentials. Classical molecular dynamics in the NVT ensemble was run for 50 ps with a time step of 0.25 fs. These simulations were performed at two temperatures, 298.2 and 5 K, the latter to clearly identify the normal modes. A total of 1000 configurations were stored for the analysis. The vibrational features of TMA that are of interest to us lie below frequencies of 800 cm^{-1}. Since the intramolecular frequencies of the methyl group are much larger than this limit, the flexibility of the methyl groups will likely not alter any of the intrinsic vibrational features of the central bridge in TMA.

The frequency spectrum at 298.2 K obtained from such an analysis is also shown in Figure 7. Since we are making a harmonic approximation to the atomic dynamics, the spectrum obtained through the normal-mode procedure may not have features at all the frequencies where the power spectrum exhibits peaks. A comparison of the peak positions found in the experimental spectra,[15,16] and those from our classical simulations are tabulated in Table 5. The atomic displacements of selected modes are shown in Figure 8. We follow refs15 and 16 for the notation used in the assignments, ν_i. In general, we find that the frequencies obtained from the empirical model are significantly higher than those obtained from spectroscopic data. Important factors that could cause this shift are the stronger binding of the methyl groups and the lack of distinction between C_b and C_t in the model in comparison to experiment.

TABLE 5: Comparison of Vibrational Properties of the Classically Modeled TMA Crystal at 223.2 K and the TMA Dimer in the Gas Phase at 298.2 K Modeled by the Car-Parrinello Method with Infrared (I) and Raman (R) Spectroscopic Data in the Far-Infrared Region[a]

peak position [cm^{-1}]			
classical simulation	CPMD	assignment	experiment[15,16]
188	150	ν_4	153 [R]
	168	ν_{12}	185 [R]
158	200	ν_7 (a)	192 [R]
193	235	ν_{15}	232 [R]
463		ν_6	274 [R]
	308	ν_3	313 [R]
474	363	ν_{17}	367 [I]
534, 594	453	ν_2	453 [R]
525		ν_{13}	479 [I]
	560	ν_{16}	565 [I]
	586	ν_1	592 [R]
	687	ν_8	696 [I]

[a] The assignments correspond to the experimental and classical simulation data.

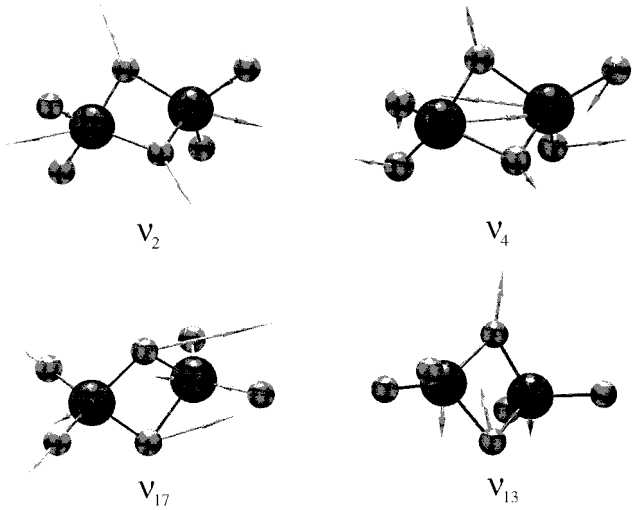

Figure 8. Atomic displacements of some of the normal modes in TMA. The assignments used can be found in refs15 and 16.

Ab Initio Studies. Various distances and angles of the energy-minimized TMA dimer obtained using the Car-Parrinello method are reported in Table 3 and compared with experimental data and results from the classical studies. The CP results agree well with experiments on almost all structural quantities, including the reproduction of a longer Al−C_b as compared to a Al−C_t bond.

The dimerization energy of TMA obtained from the CPMD total energies of minimized configurations of the dimer and monomer is found to be 54.4 kJ/mol compared to the experimental estimate of 95 kJ/mol given above. Previous Hartree−Fock calculations gave a significantly lower dimerization energy for TMA.[18] Both of the estimates are likely to be lower bounds due to the neglect of dispersion forces.

The power spectrum of the velocity autocorrelation function of atoms in TMA obtained from the CPMD run is shown in Figure 9. Important spectral features are tabulated in Table 5.

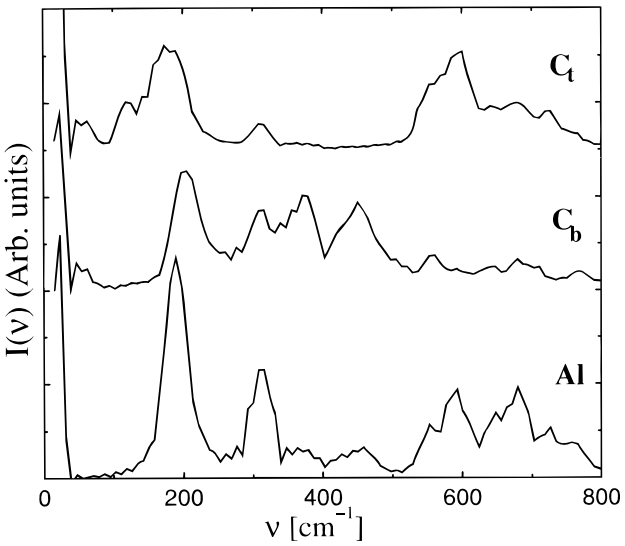

Figure 9. Power spectra of aluminum, bridging, and terminal carbons for the CPMD run at 400 K. The spectra were smoothened by a three-point sampling method.

It is seen that the CPMD results are much closer to experiments than those obtained from simulations with an empirical potential. Experimentally, the IR-active, bridge-sharing mode, ν_{17} (see Figure 8 for an illustration), is observed at 367 cm^{-1}. In Figure 9, it can be seen that at this frequency, the power spectrum for the terminal carbons is featureless around this frequency range while that for the aluminum and bridging carbons exhibit a peak. The frequencies obtained from the CPMD simulations are consistently red-shifted when compared to experiment by about 10 cm^{-1}. This is typical of the density functional approximation.

5. Conclusions

We have performed both classical MD and ab initio CPMD simulations on trimethylaluminum. A simple empirical interaction potential between aluminum and the rigid methyl group was obtained from potentials existing in the literature and was modified for modeling TMA. Overall, results from this potential compare favorably with experimental data on the condensed phases of TMA, although the model is unable to reproduce subtle structural and dynamical features. Further improvements in this model will need to incorporate effects of polarizability, in particular, to obtain bonding within the bridge of the TMA dimer correctly.[19,20] The classical dimer simulations have been complemented by CPMD simulations, which are shown to provide a surprisingly accurate picture of the structure and dynamics. However, the dimerization energy obtained from the CPMD method is found to be somewhat lower than the experimental value. The reason is possibly due to the choice of gradient correction and the lack of an adequate treatment of the dispersion interaction, which is an inherent feature of the current generation of density functional schemes.

Acknowledgment. We thank Glenn Martyna and Mark Tuckerman for providing the PINY-MD code. Discussions with Preston Moore and Ken Bagchi provided insight for the normal-mode analysis. We thank Kari Laasonen, Gary Zhao, Karl Wiegand, Jeff Books, Sam Sangokoya, and Dixie Goins for informative discussions. This work was supported by the Albemarle Corp. and by the National Science Foundation Grants Nos. NSF CHE 96-23017 and NSF DMR 96-32598.

References and Notes

(1) Eisch, J. J. In *Comprehensive Organometallic Chemistry II*; Abel, E. W., Stone, F. G. A., Wilkinson, G., Eds.; Pergamon: New York, 1995; Vol. I, p 431.
(2) Reddy, S. S.; Sivaram, S. *Prog. Polym. Sci.* **1995**, *20*, 309.
(3) Sinn, H.; Kaminsky, W.; Vollmer, H. J.; Woldt, R. *Angew. Chem., Int. Ed. Engl.* **1980**, *92*, 390.
(4) Mason, M. R.; Smith, J. M.; Bott, S. G.; Barron, A. R. *J. Am. Chem. Soc.* **1993**, *115*, 4971.
(5) Parkins, A. W.; Poller, R. C. *An introduction to organometallic chemistry;* Oxford University Press: New York, 1986.
(6) Lewis, P. H.; Rundle, R. E. *J. Chem. Phys.* **1953**, *21*, 986.
(7) Vranka, R. G.; Amma, E. L. *J. Am. Chem. Soc.* **1967**, *89*, 3121.
(8) Longuet-Higgins, H. C. *J. Chem. Soc.* **1946**, 139.
(9) Pitzer, K. S.; Gutowsky, H. S. *J. Am. Chem. Soc.* **1946**, *68*, 2204.
(10) Laubengayer, A. W.; Gilliam, W. F. *J. Am. Chem. Soc.* **1941**, *63*, 477.
(11) Elschenbroich, C.; Salzer, A. *Organometallics: A concise introduction;* VCH: Weinheim, Germany, 1992.
(12) Almenningen, A.; Halvorsen, S.; Haaland, A. *Acta Chem. Scand.* **1971**, *25*, 1937.
(13) Muller, N.; Pritchard, D. E. *J. Am. Chem. Soc.* **1960**, *82*, 248.
(14) Ramey, K. C.; O'Brien, J. F.; Hasegawa, I.; Borchert, A. E. *J. Phys. Chem.* **1965**, *69*, 3418.
(15) Hoffmann, v. E. G. *Z. Electrochem.* **1960**, *64*, 616.
(16) Onishi, T.; Shimanouchi, T. *Spectrochim. Acta* **1964**, *20*, 325.
(17) Chey, J.; Choe, H. S.; Chook, Y. M.; Jensen, E.; Seida, P. R.; Franci, M. M. *Organometallics* **1990**, *9*, 2430.
(18) Tarazona, A.; Koglin, E.; Buda, F.; Coussens, B. B.; Renkema, J.; van Heel, S.; Meier, R. J. *J. Phys. Chem.* **1997**, *101*, 4370.
(19) Wilson, M.; Madden, P. A.; Costa-Cabral, B. J. *J. Phys. Chem.* **1996**, *100*, 1227.
(20) Rick, S. W.; Stuart, S. J.; Berne, B. J. *J. Chem. Phys.* **1994**, *101*, 6141.
(21) Tsuneyuki, S.; Tsukada, M.; Aoki, H.; Matsui, Y. *Phys. Rev. Lett.* **1988**, *61*, 869.
(22) van Beest, B. W. H.; Kramer, G. J.; van Santen, R. A. *Phys. Rev. Lett.* **1990**, *64*, 1955.
(23) Williams, D. E. *J. Chem. Phys* **1967**, *47*, 4680.
(24) Martyna, G. J.; Tuckerman, M. E.; Tobias, D. J.; Klein, M. L. *Mol. Phys.* **1996**, *87*, 1117.
(25) Car, R.; Parrinello, M. *Phys. Rev. Lett.* **1985**, *55*, 2471.
(26) Galli, G.; Parrinello, M. In *Computer simulations in material science*; Meyer, M., Pontikis, V., Eds.; Kluwer: Boston, 1991.
(27) Remler, D. K.; Madden, P. A. *Mol. Phys.* **1990**, *70*, 691.
(28) Tuckerman, M. E.; Parrinello, M. *J. Chem. Phys.* **1994**, *101*, 1302.
(29) Troullier, N.; Martins, J. L. *Phys. Rev. B* **1991**, *43*, 1993.
(30) Becke, A. D. *Phys. Rev. A* **1988**, *38*, 3098.
(31) Lee, C.; Yang, W.; Parr, R. G. *Phys. Rev. B* **1988**, *37*, 785.
(32) Tobias, D. J.; Martyna, G.; Klein, M. L. *J. Phys. Chem.* **1993**, *97*, 12959.
(33) A tabulation of the liquid TMA versus temperature; Albemarle Corp.; Baton Rouge, LA, 1959 (unpublished).
(34) Gezelter, J. D.; Rabani, E.; Berne, B. J. *J. Chem. Phys.* **1997**, *107*, 4618.